

A new model of fuel spray shape at early stage of injection in a marine Diesel engine

Abstract. The macrostructural parameters of fuel spray atomized with an injector from a marine 4-stroke Diesel engine are determined. The fuel was injected into a constant volume chamber providing an optical access. The sprays inside the chamber were visualized by means of the Mie scattering method. The marine injector was fueled by diesel oil at a constant temperature through the common rail system. The impact of ambient conditions and the geometrical parameters of the injector on the macrostructural parameters of the fuel spray was studied. The experimental results are used to propose a modified model of spray tip penetration in early stage of fuel delivered by the marine injector. The proposed model has a lower error, about 15%-34%, than the model of Hiroyasu and Arai. Moreover a new model of the evolution over time of the spray cone angle is developed.

1 Introduction

Diesel engines are commonly used sources of mechanical energy on ships. Typically, there are low-speed two-stroke diesel engines and medium-speed four-stroke ones. The source of energy in such engines is the combustion process of diesel oil or heavy fuel oil. Due to the large dimensions of marine engines and long periods of operation (many weeks of continuous operation), the air pollution may be considerable. The International Maritime Organization (IMO) has established the Marine Environment Protection Committee (MEPC), which has determined limitations on the amount of sulfur in fuel that is acceptable for the Sulphur Emission Control Area (SECA). These limitations are too low to allow the use of high fuel oil (HFO) in these SECAs. Therefore, marine diesel oil (MDO) is used. It should be noted that a marine engine with a nominal power of 10 MW consumes 48 tonnes of fuel per day (on the assumption that the specific fuel consumption is 200 g/kWh). Due to the significant air pollution and high costs of operating marine engines as a result of fuel consumption, engineers and scientists must improve the in-cylinder processes so that the combustion is cleaner and more efficient.

The combustion process in a diesel engine cylinder is mainly determined by the fuel injection process (Zhou *et al.*, 2019). Fuel delivered by the injector is atomized and simultaneously evaporated and mixed with air/exhaust gas mixture and burnt. According to Payri *et al.* (Payri *et al.*, 2015), five phases may be observed in fuel tip propagation: (I) non-reaction, (II) auto-ignition expansion, (III) stabilization, (IV) acceleration, and (V) quasi-steady propagation. The first phase is usually divided into two stages: primary and secondary break-up (Hiroyasu and Arai, 1990). Fuel is delivered and atomized to the cylinder under high pressure. The atomized fuel creates a cloud of droplets in a conical shape. The conical cloud of droplets is described by two main parameters: spray tip penetration (STP) and spray cone angle (SCA) (Figure 3.) and micro-parameters such as Sauter Mean Diameter (SMD) or the average droplet diameter. It has been

30 shown that these phenomena are determined by the dimensions of the fuel nozzle holes, the fuel flow, the pressure in the
31 engine cylinder, and the properties of the fuel.

32 In the literature, there are many studies numerical and experimental concerning the parameters of fuel injection depending
33 on the injection pressure (Chen *et al.*, 2019; Lei *et al.*, 2019; Vaid *et al.*, 2014), backpressure (ambient pressure in the
34 engine cylinder)(Jing *et al.*, 2017; Payri *et al.*, 2009, 2017), and shape of the nozzle holes (Wang *et al.*, 2015) including
35 their conicity, which is defined by the K factor (Feng *et al.*, 2016; Som *et al.*, 2011), $K = 1$ for cylindrical holes. According
36 to results obtained by Payri *et al.* (Payri *et al.*, 2008), an increase of the K factor causes an increase of the SCA. The
37 method of fuel injector activation affects the parameters of the fuel spray as well. In (Yu *et al.*, 2017) and (Suh *et al.*,
38 2007), measurement results for piezo- and solenoid-driven fuel injectors were presented. The energizing of the fuel
39 injector by a piezoelectric system with a fuel injection pressure of 60 MPa causes lower tip penetration and a higher SCA
40 compared to energizing by a solenoid system. An analysis of adjacent fuel injection holes (Nishida *et al.*, 2009) is also
41 available. Most researchers assume that the break-up process is determined by cavitation phenomena on the rough surfaces
42 of the nozzle holes (Liu *et al.*, 2018; Wang, 2013). Most researches are limited to the injection process of the general
43 Diesel engine. Therefore, the injection system and fuel spray parameters of marine diesel engine with the large nozzle
44 length/diameter (L/D) with operating parameters the same as in a marine diesel engine is studied rarely. The cavitation
45 phenomena is important design criterion of the fuel injection system and spray characteristics in marine Diesel engines.
46 Yan *et al.* (Yan *et al.*, 2016) studied effect of injection pressure on cavitation and spray in marine diesel engine. In this
47 studied was used to simulate cavitation and spray two – phase flow model combined with single bubble dynamics and a
48 droplet break-up model. The numerical simulation results was compared to the experimental data. In the research of
49 marine injectors, an increasing development of numerical simulation test is observed. Balz R.(Balz *et al.*, 2021) and all
50 presents numerical and experimental investigation of cavitation in marine Diesel injectors. They showed that,
51 experimental in-nozzle flow visualization has shown cavitation patterns in the nozzle bore. It is determined that, the
52 geometric characteristics of nozzle bore location and its direction have a dominant effect on the type and evaluation of
53 cavitation formation. The additional have been executed CFD simulation results in order to validation results. With the
54 development of research on alternative fuels, there are a lot of studies on the characteristics of the fuel spray and
55 combustion of fuels other than diesel (Adamczyk *et al.*, 2020; Cai and Abraham, 2017; Yu, 2019).

6 It should be emphasized that the available publications concerning fuel injectors and injection conditions usually treat
7 those occurring in diesel engines with small dimensions compared to marine engines (Kostas *et al.*, 2009). According to
8 Kowalski (Kowalski, 2014), the diameter of the nozzle holes in marine fuel injectors is commonly larger than 0.3 mm.
9 The fuel injection pressure is similar at 40 MPa (except for common rail systems) and the backpressure exceeds 4 MPa
0 at the instant of injection. The largest observed diameter of a nozzle hole (0.3 mm) is presented in (Lee and Park, 2002),
1 but under higher fuel injection pressure. The parameters of the fuel spray are determined using mathematical models

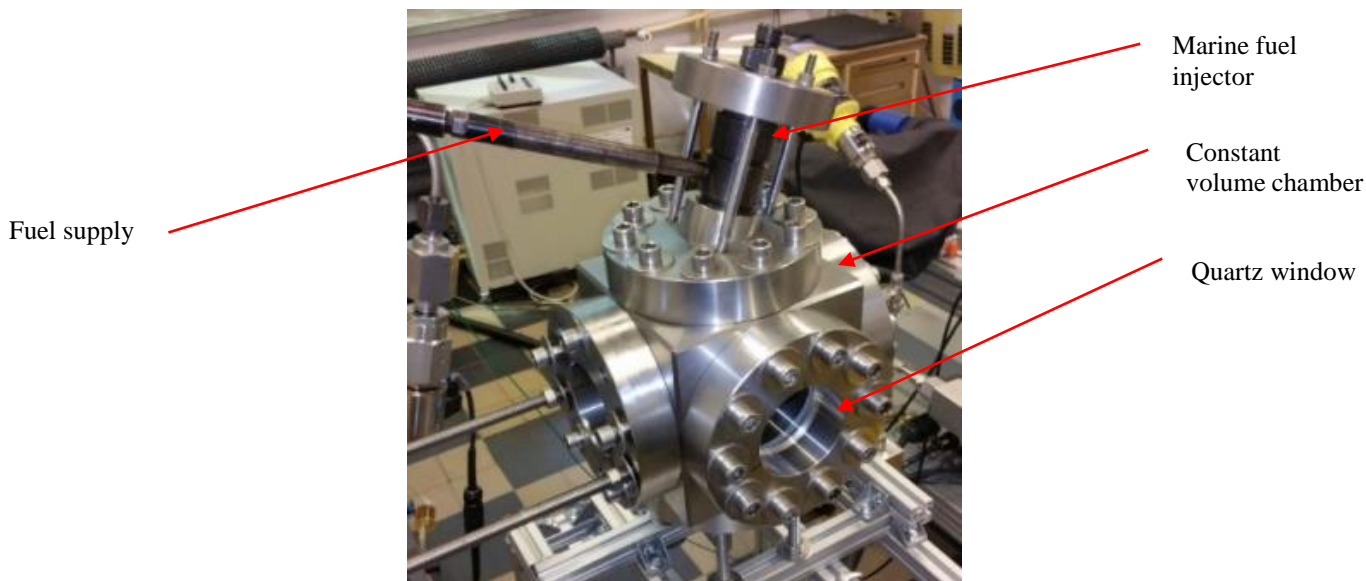
62 presented in the literature. The many developed models of diesel STP are elaborated based on the assumptions made by
63 Hiroyasu and Arai (Hiroyasu and Arai, 1990) or Naber and Siebers (Naber and Siebers, 1996). The fuel atomization
64 model of Hiroyasu and Arai is used for the analysis of experimental research and the rating of the validity their results.
65 This model assumes that STP is linearly proportional to the time only in the early injection period. The values of the
66 various spray parameters depend on time, ambient gas density, backpressures and differences in fuel specifications. After
67 the period of time in which the STP has a linear proportionality, it has been found to be proportional to the square root of
68 the elapsed time. In the period of time in which it is proportional to the square root of the elapsed time, geometrical
69 parameters of the fuel nozzle, such as the diameter, must be taken into account. The other models of fuel STP described
70 in the literature are similar to that of Hiroyasu and Arai and are in general two-step (Bohl *et al.*, 2017; Kostas *et al.*, 2009)
71 including t_B . According to these models, the initial step before t_B does not include the geometrical parameters of the fuel
72 nozzle. But usually SCA and STP are measured for fully developed spray (Bohl *et al.*, 2017; Hiroyasu and Arai, 1990;
73 Reitz and Bracco, 1979). In a marine diesel engine, the start of combustion is much earlier (Kowalski, 2016). Hence, the
74 present authors believe that the description of the early stage of fuel spray is most important to understand and describe
75 the combustion process in the engine cylinder. The second novelty area, in comparison to other works, is the finding of a
76 dependence between the geometrical parameters of the fuel nozzle and the fuel spray geometry at the early stage of
77 injection. This problem is omitted in the model of Hiroyasu and Arai and other models.

78 The main target of the present paper is to propose a new model of STP and SCA for large injectors. On the basis of
79 experimental research, new models are proposed for the early stage of fuel spray, taking into account the geometry of a
80 large fuel injector. The model is obtained on the basis of experimental results and a modification of the Hiroyasu and Arai
81 model.

82 **2 Laboratory setup**

83 The research was conducted in a constant-volume chamber with a quartz window providing 100-mm optical access
84 (Figure 1.) (Grochowalska, 2019). The injector used is a conventional pressure-opened diesel injector from a Sulzer AI
85 25/30 type marine engine equipped with a Unit Pump injection system. The injector was located at the top of the chamber.
86 This setup allows observing the evolution of a single fuel jet at a distance of almost 100 mm (half of the cylinder bore).
87 The fuel was supplied to the injector by a high-pressure common rail system equipped with a fast-acting electromagnetic
8 valve releasing fuel flow to the injector. The pressure behind the injector was measured by means of a Kistler type 4067E
9 (Kistler, 2014) piezoresistive pressure sensor.

0 The spray inside the chamber was observed by means of the Mie scattering technique (Grochowalska, 2019; Piazzullo
1 *et al.*, 2017). The spray was illuminated in a visible range of wavelengths as in Zigan *et al.* (Zigan *et al.*, 2011). Mie
2 scattering results may differ greatly depending on the type of spray illumination.



93

94

Figure 1. Constant-volume chamber with injector on the top (Grochowalska, 2019)

95

Light sheet illumination is necessary when visualizing hollow cone sprays. As far as cylindrical nozzle sprays are concerned, the integral type of illumination performs very well, especially in the determination of global spray parameters.

96

In this study, both SCA and STP were determined and therefore the integral illumination of the spray was chosen. For

97

this purpose, two externally located halogen lights (0.5 kW each) were used. The illuminated sprays were observed by a

98

Photron SA1.1 high-speed camera. The resolution of the recorded images was 512×256 pixels. The images were recorded

99

at a frequency of 40 kHz. A schematic of the experimental setup is shown in Figure 2.

100

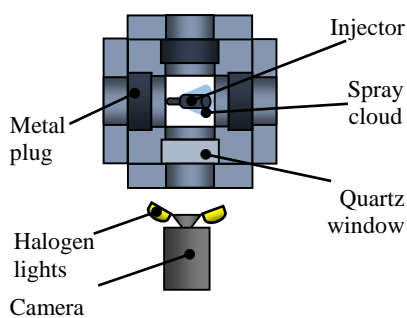


Figure 2. The experimental setup

101

102

103

104

5

6

7

8

9



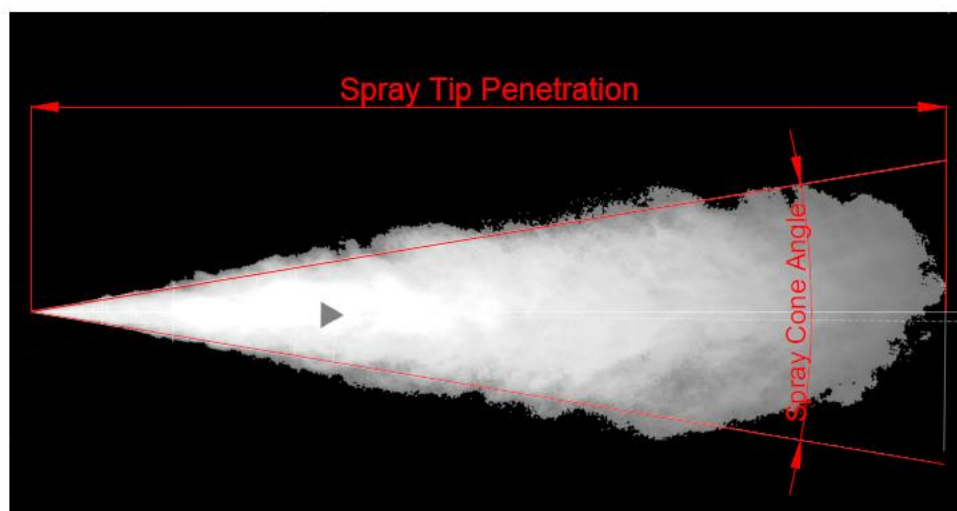
110 **Table I.** Nozzle parameters

	Diameter (D) [μm]	Ratio $\frac{L}{D}$	K factor (Som <i>et al.</i> , 2011)
Nozzle 1	285	10.9	1
Nozzle 2	325	9.5	1
Nozzle 3	375	8.3	1

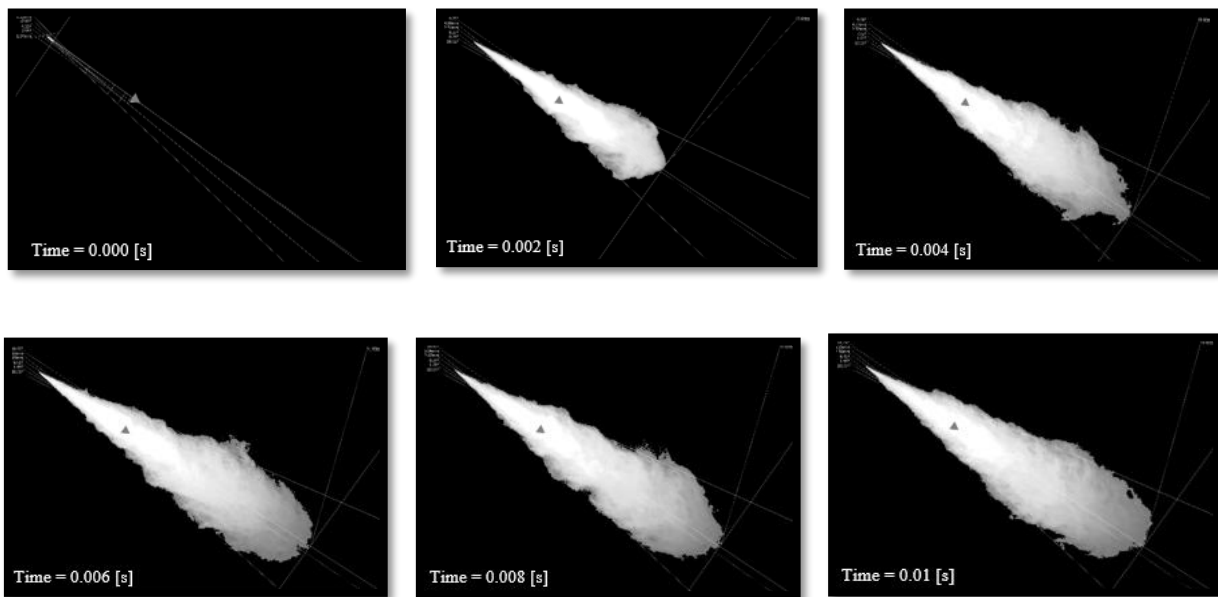
111 The injection process was tested for three different nozzle diameters. The ratio $\frac{L}{D}$ (L is the length of the nozzle and D is
 112 its diameter) is presented in Table I. The fuel pressure in the common rail system was 50 MPa. The injector opening
 113 pressure was adjusted to 25 MPa (the same as in the Al 25/30 marine engine). Each nozzle was tested at two different
 114 backpressures: 3.2 and 4.3 MPa, corresponding to half- and full-load engine operation, respectively. The measurement
 115 was repeated three times at each point. The temperature during the test was 300 K. The measured diesel oil viscosity and
 116 density were equal to 2.35 mPa*s and 816.1 kg/m³, respectively, at 40 °C. The obtained images were processed by DaVis
 117 v8.4 software.

118 3 Results and discussion

119 Figure 3 presents an example of the resulting macro-parameters of the tested diesel spray. STP is defined as the
 120 distance from the nozzle to the front of the spray (Feng *et al.*, 2016; Heywood, 1988). According to the presented results,
 121 the spray direction is determined by three lines: two on the boundaries on the left and right sides and the third being the
 122 line of the nozzle symmetry. Interpolation of the left and right sides of the boundary was performed.



3
4 **Figure 3.** Schematic of diesel fuel spray defining its macro-parameters



125

126

127 **Figure 4.** Mie scattering spray image for nozzle 2 with a backpressure of 4.3 MPa

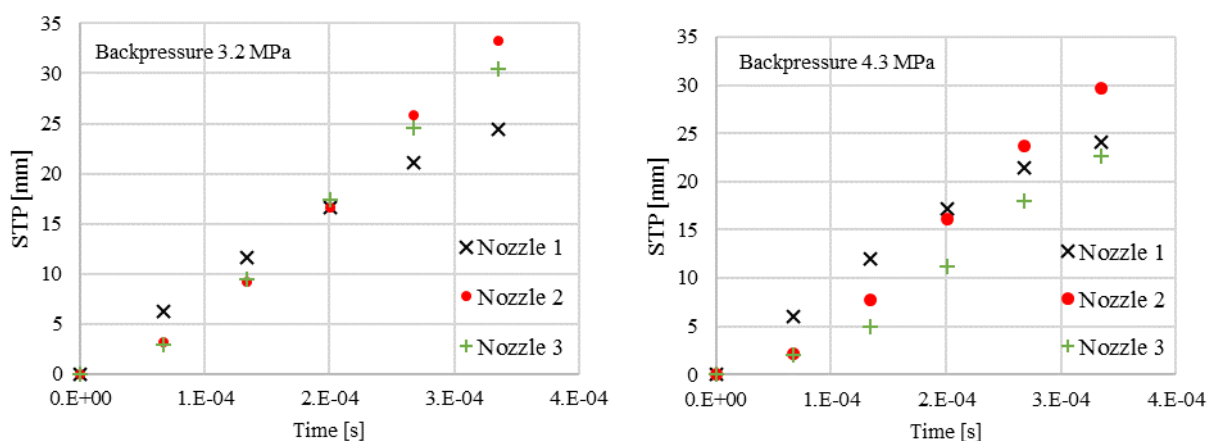
128 The analysis of the macrostructure of the fuel spray was conducted using 250 frames for each injection process, which
 129 covered the range from the beginning of the injection to the complete development of the spray. Figure 4 shows selected
 130 images presenting the development of the diesel fuel spray for nozzle 2 with a backpressure of 4.3 MPa. The
 131 measurements and received series of images depicting the diesel spray from the injector were recorded. Prior to the
 132 calculation of the macro-parameters of the diesel spray, pictures had to be prepared. The first stage of image processing
 133 was scaling from pixels to millimeters with verification of the nozzle position in the picture. One pixel is equal to 0.13
 134 mm in this study. Secondly, the spray isolator function was used to separate the spray from the ambient and to eliminate
 135 reflections and image noises within a short distance from the spray. The prepared series of images was used to define the
 136 STP and SCA, and propose a new model for these parameters.

137 3.1 Spray Tip Penetration

138 Figure 5 presents the results of the STP measurements. The presented test results are the arithmetic mean of three
 139 observations of the measurement and are qualitatively similar to the results presented in (Cai and Abraham, 2017; Siebers,
 140 1999). Comparing these with the results of combustion in the AL25/30 engine from (Kowalski, 2014) it should be noted
 141 that the start of combustion is when the cloud of the fuel spray is not fully developed. These charts contain data only up
 2 to 0.0004 s (the cloud of the fuel spray is not fully developed). According to Siebers (Siebers, 1999), the maximum STP
 3 of fuel spray increases linearly with the increasing of nozzle diameter. This trend was observed in experimental results in
 4 the early stage of STP.

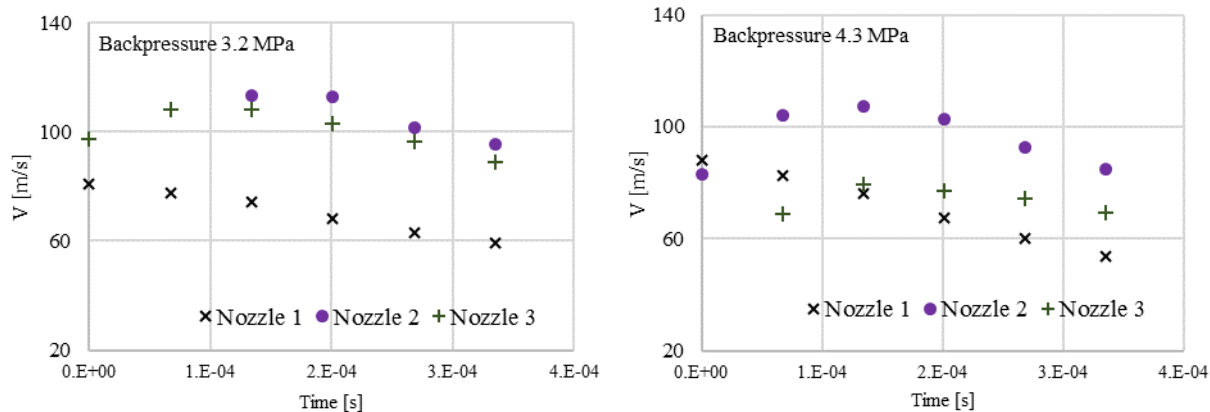
5 In the standard combustion chamber conditions the maximum liquid spray distance is limited by hot air entrainment rate
 6 and mixing of fuel and air (Siebers, 1999). First of all, the energy needed for evaporation of the fuel results from the high
 7 ambient temperature in the cylinder of a diesel engine. The above evaporation is influenced by nozzle diameters, hot air

148 entrainment rate and properties of the fuel. A decrease of the nozzle diameter causes a reduction of the size of the fuel
 149 droplets produced and lowers their speed. This finding was presented in the test results in (Som *et al.*, 2011). It is important
 150 to mention that decreasing $\frac{L}{D}$ (the increase of the nozzle diameter in this case) may cause a turbulent flow inside the nozzle
 151 and cavitation (Yao *et al.*, 2016) which could also influence the results obtained here. Naturally, when the distance from
 152 the nozzle increases, the diameters of the droplets in the fuel spray decrease (Yu, 2019). As ambient gas density increases,
 153 spray dispersion increases, which results in more entrained air particle in the spray. The larger entrained mass leads to a
 154 slower penetration velocity based on conservation of momentum, and therefore, reduced penetration (Balz *et al.*, 2020).
 155 This is caused by the aerodynamic resistance in the constant volume chamber (secondary break-up). The influence of
 156 increasing backpressure on reducing the STP was shown in (Grochowalska, 2019; Payri *et al.*, 2017; Wang *et al.*, 2016)
 157 and (Yan *et al.*, 2016) and are confirmed by the present results. On the basis of the analysis in Figure 5 and (Grochowalska,
 158 2019), it may be concluded that an increase of backpressure generally causes a reduction of STP for big nozzles. The
 159 reason for this is the formation of large droplets at the exit of the fuel injector nozzle about the big diameter of the outlet
 160 nozzle. The large droplets break up longer in time under the influence of backpressure, but also have a higher growth rate
 161 at the very beginning compared to the diameter droplets formation by the smaller diameter of the outlet nozzle. The higher
 162 growth rate of STP was shown in Figure 6. The growth rate of STP was particularly higher for a big nozzle at a
 163 backpressure of 3.2 MPa than at 4.3 MPa. It should be noted that the working space of the constant volume chamber was
 164 filled with nitrogen. As is well known, nitrogen has a lower density than oxygen contained in the air. Therefore, the
 165 experimental results of STP are valid only for the considered condition.



166
 7 **Figure 5.** STP for the nozzles 1, 2, and 3 with backpressures of 3.2 MPa and 4.3 MPa
 8
 9





170

171 **Figure 6.** Growth rate of STP for backpressures of 3.2 MPa and 4.3 MPa

172 **3.1.1 Model for spray tip penetration**

173 The temporal development of the STP in the combustion chamber of diesel engines has been examined and
 174 described for many years. Generally, many correlations come from the work of Hiroyasu and Arai (Hiroyasu and Arai,
 175 1990). These correlations were used for comparison purposes in this paper. The Hiroyasu and Arai model was verified at
 176 low injection pressure and backpressure. Therefore, the theoretical correlations were believed appropriate in analysis of
 177 the dependencies of the spray parameters of a marine diesel engine. Hiroyasu proposed that during the early stage of fuel
 178 injection the spray penetration is proportional to time [linear stage (1)], while at later stages it is proportional to the square
 179 root of the time (2). The time when the transition occurs is referred to as the breakup time t_b (3). The Hiroyasu and Arai
 180 model is presented in the form:

181
$$STP(t) = 0.39 \sqrt{\left(\frac{2\Delta P}{\rho_f}\right)} t \dots 0 < t < t_b \quad (1)$$

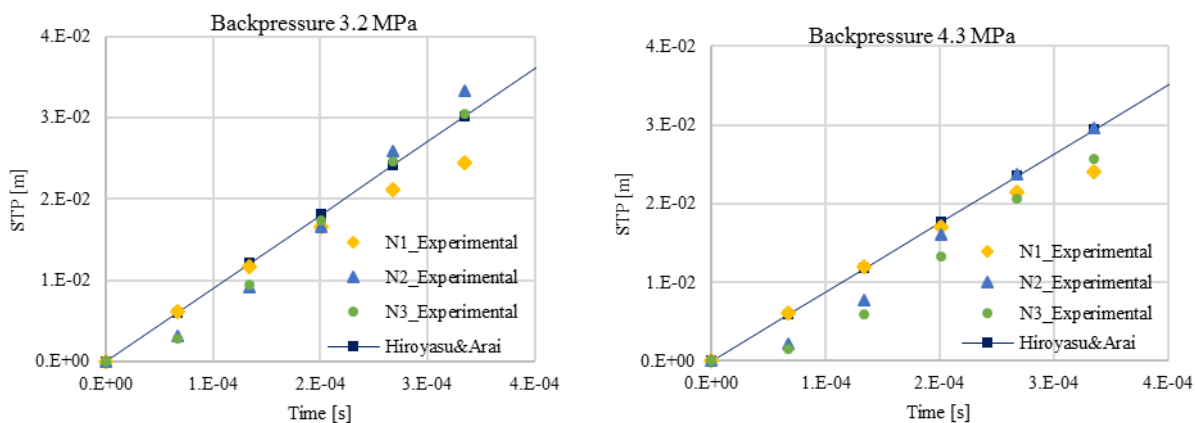
182
$$STP(t) = 2.95 \left(\frac{\Delta P}{\rho_f}\right)^{\frac{1}{4}} \sqrt{(Dt)} \dots t > t_b \quad (2)$$

183
$$t_b = 29 \frac{\rho_f D}{(\rho_a \Delta P)^{0.5}} \quad (3)$$

184 STP (t)- STP (m), ΔP – difference between fuel pressure in the nozzle and the ambient pressure (Pa), ρ_f -fuel density
 185 (kg/m^3), D-nozzle diameter (m), t-time (s).

186 According to the results presented in Figure 5, a linear model of STP may be adopted from the start of injection (SOI) to
 7 (2.0-3.4) $\times 10^{-4}$ s, depending on the backpressure and nozzle diameter (time t_b). A smaller nozzle diameter and higher
 8 backpressure cause a decrease in t_b . According to the Hiroyasu and Arai model, the STP at the beginning of the injection
 9 does not depend on the nozzle diameter, but the measurement results show that this is not true. The initial stage of the
 0 experimental evolution of STP for all cases is very similar but not the same. Figure 5 shows the STP of the initial stage
 1 in the charts up to 0.0004 s, in which it can be seen that there are differences, as depicted. Geometrical parameters such
 2 as the length to diameter ratio of the fuel nozzle have a significant effect on the STP in the considered nozzles. The

193 influence of this ratio on liquid length spray penetration was found by Siebers (Siebers, 1999) who found a linear relation
 194 between the nozzle hole diameters and liquid spray penetration, but only for fully developed fuel spray. The early stage
 195 STP model of Hiroyasu and Arai does not include changes in the nozzle diameter, but only the difference between the
 196 fuel injection pressure and backpressure. As one of the main parameters of influence on the STP of fuel spray there is the
 197 difference between the pressure into the nozzle and the backpressure in the constant volume chamber, which was included
 198 in the Hiroyasu and Arai model. Therefore, in the presented experimental tests, the fuel pressure in the fuel line was
 199 measured. The diesel fuel pressure was maintained by a fuel pump. The fuel pressure sensor was located in the fuel line
 200 in front of the fuel injector (Section 2 *Laboratory setup*). The fuel pressure before the exit nozzle is equal to the fuel line
 201 pressure. Opening the fuel injector caused fuel to flow and temporarily change the pressure in the fuel line to be the same
 202 as in the nozzle. At first there follows a sharp rises of the fuel pressure, which then becomes stable. The temporary fuel
 203 pressure change in the fuel line and fuel spray propagation in the constant volume chamber continued simultaneously. In
 204 (Lei *et al.*, 2019) there was presented research about the effect of the injection behavior on fuel spray penetration,
 205 confirming the influence of the fuel pressure on the characteristics of the spray. Therefore pressure changes should be
 206 taken into consideration. Figure 7 presents the early stage of the experimental data of STP to time 0.0004 ms of the
 207 development of the fuel spray and the Hiroyasu and Arai model based on the experimental input data.



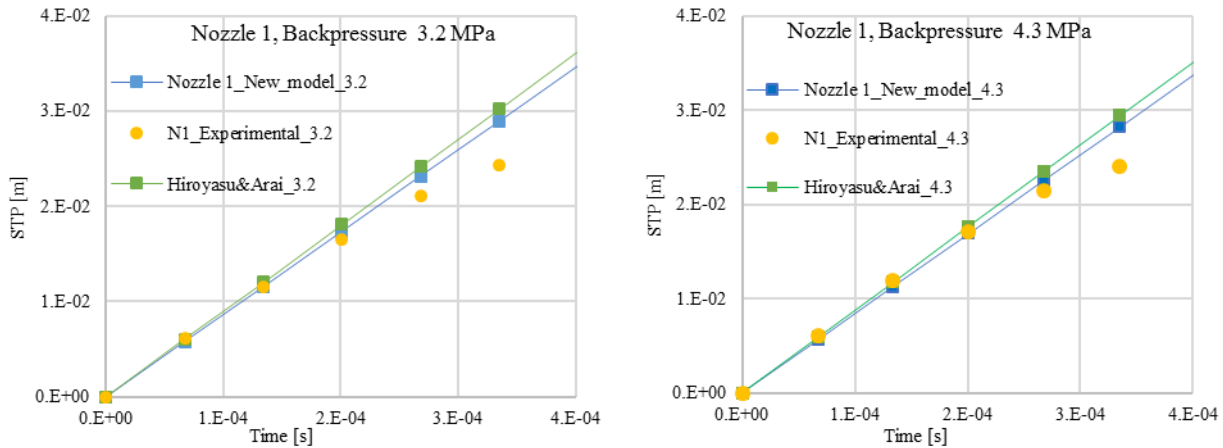
208
 209 **Figure 7.** Early stage of the experimental data of STP and Hiroyasu and Arai model on based experimental input data

210 In Figure 7 there can be observed differences between the experimental results and the Hiroyasu and Arai model for the
 211 considered backpressures. The average relative error between the experimental results and the Hiroyasu and Arai model
 2 is in the range 19%-38% (Figure 9). Therefore, it can be suggested that a mathematical model of linear STP should be
 3 extended to include the influence of the nozzle diameters. The present analysis shows that Equation 1 of the Hiroyasu and
 4 Arai model should be extended for the considered experimental results to the following form:

$$5 \quad STP(t) = 0.0641 \cdot \left(\frac{L}{D} + 1\right) \sqrt{\left(\frac{2\Delta P}{\rho_f}\right)} \cdot t \quad (4)$$

216 • ratio $\frac{L}{D}$, L- nozzle length [m], D – nozzle diameter [m];

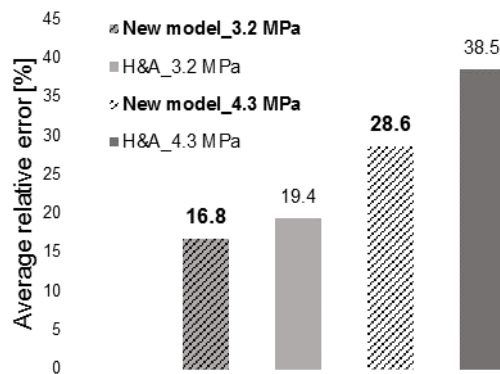
217 Examples of the results of the new model of the STP for Nozzle 1 are presented in Figure 8.



218
219 **Figure 8.** Early stage of the STP for new model, experimental data and Hiroyasu and Arai model

220 The results of the modified model for STP agree with the experimental data. By introducing the ratio $\frac{L}{D}$ it is possible to
221 adjust the model results to the experimental data for different nozzle geometries in the early stage of injection.

222 Figure 9 presents the calculated relative errors of the Hiroyasu and Arai model and the proposed STP model for the early
223 stage of injection in comparison to the experimental results. A general analysis shows that the proposed model gives a
224 lower average error in relation to the experimental results compared with the Hiroyasu and Arai model. The decrease of
225 the mentioned error is about 15%-34% for the considered parameters in dependence on the fuel nozzle geometry.

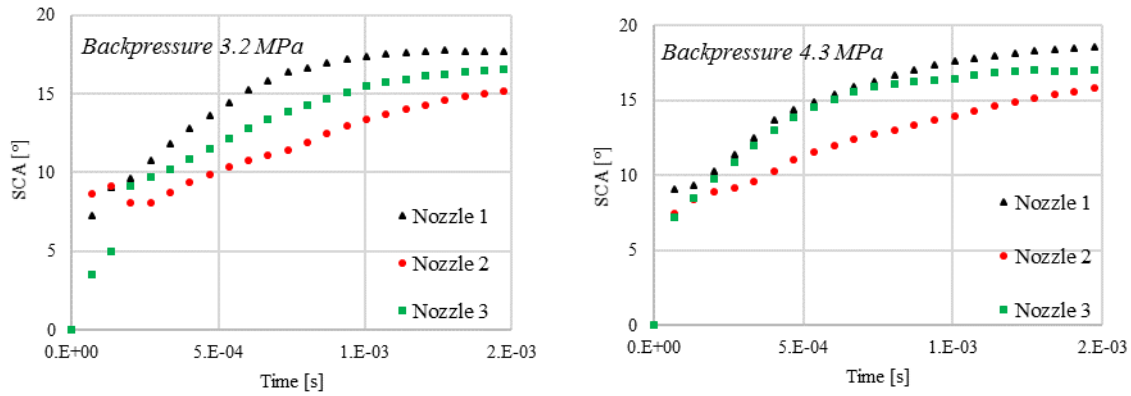


226
227 **Figure 9.** Average relative error between experimental of STP and new model of STP for all considered nozzles

3.2 Spray cone angle

0 Figure 10 presents the evolution of the SCA with time for the considered nozzles and backpressures. In the early stage
1 (from the SOI up to 0.001 s), the increase of the SCA can be observed for all of the tested nozzles. The value of the
2 maximum SCA for diesel oil and different diameters of nozzles changes in a range of about 16°–20°. Nevertheless,

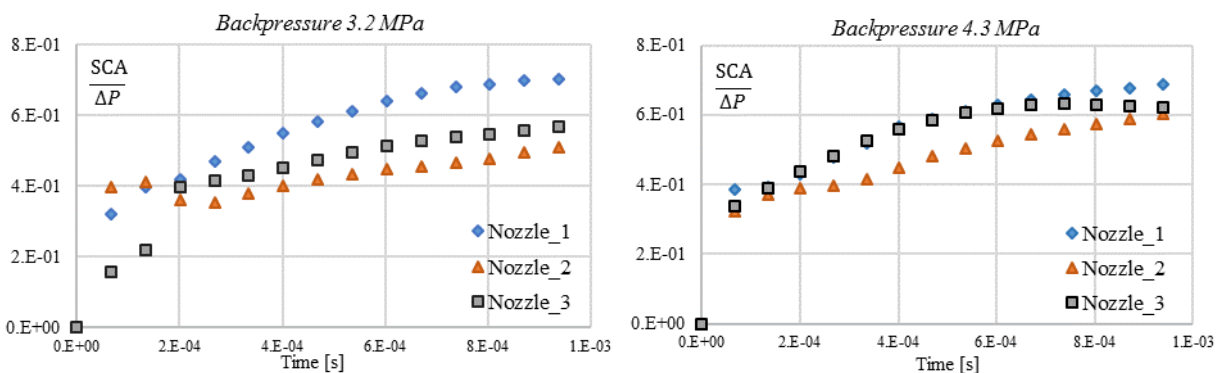
233 depending on the geometrical parameters of the injector nozzle, the growth rate of the SCA differs. When the nozzle
 234 diameter is increased and $\frac{L}{D}$ is decreased, it is possible to observe a decrease of the SCA at all considered backpressures,
 235 as shown in Figure 10. This is probably caused by the need for a longer time for the break-up and partial evaporation of
 236 the droplets produced by nozzles with bigger diameters.



237

238 **Figure 10.** SCA for considered nozzles 1, 2, 3 and backpressures

239 The influence of the backpressure on the SCA was also observed. This is confirmed by (Feng *et al.*, 2016) and Figure 10.
 240 This is particularly observed for big nozzles of a fuel injector. An increased density of the surrounding gas causes a higher
 241 growth in the radial direction than in the axial one. As mentioned before, the difference between the fuel pressure and the
 242 backpressure influences the fuel spray. Therefore, Figure 11 shows the course over time of SCA in dependence on the
 243 difference between the injection pressure of the fuel injector and the backpressure into the constant volume chamber (ΔP).
 244 It should be noted that the injection pressure was changed in time, but the backpressure was almost constant.



5

6 **Figure 11.** (SCA/ ΔP) ratio over time for considered nozzles and backpressures

7 Additionally, the value of the SCA may be influenced by cavitation occurring at the end of the nozzle (Balz *et al.*, 2020).
 8 The formation of cavitation bubbles at the exit of the nozzle may cause greater dissipation and an increase of the value of
 9 the SCA (Sou *et al.*, 2007). For nozzles 2 and 3 there was observed a significant effect of a change in the difference

250 between the pressures on the SCA in time (Grochowalska, 2019). This is related to the formation of large droplets in the
 251 fuel spray at the beginning and the aerodynamic resistance in the constant volume chamber. An increase of backpressure
 252 in the constant volume chamber caused a decrease in the influence of the difference between the pressures on SCA for
 253 nozzle 2 and nozzle 3.

254 Generalizing this observation, a change in the fuel pressure in the fuel line over time in relation to the
 255 backpressure on the exit injection nozzle has an influence on the SCA. This influence on the SCA decreases over time.
 256 The second observation is that an increase of the backpressure on the exit of the fuel nozzle causes a decrease in the
 257 influence of the pressure change on the value of the SCA over time.

258 3.2.1 Model for the Spray Cone Angle

259 The existing mathematical models for SCA represent constant angles through the whole time of the development
 260 of the spray (Heywood, 1988; Kegl and Lešnik, 2018; Reitz and Bracco, 1979). The models in the literature include some
 261 characteristics of the nozzle and parameters of the injection process, fuel properties and spray environmental conditions.
 262 In the present paper, the Hiroyasu and Arai model of the SCA was selected for comparison with the experimental data.
 263 That model was presented in Equation (5), and Table II presents the SCA for the experimental and calculated results.

$$264 \quad SCA = 83.5 \left(\frac{L}{D}\right)^{-0.22} \cdot \left(\frac{D_0}{D_{sac}}\right)^{0.15} \cdot \left(\frac{\rho_g}{\rho_f}\right)^{0.26}, \quad (5)$$

265 Where: D_{sac} – the diameter of injector sac;

266 **Table.II** SCA [°] by Hiroyasu and Arai Model and experimental data

Nozzle	Backpressure 3.2 MPa (H&A model)	Experimental Average 3.2 MPa	Backpressure 4.3 MPa (H&A model)	Experimental Average 4.3 MPa
1	12.97	17	14.00	19
2	13.63	16	14.71	18
3	14.34	17	15.49	17

267 The experimental SCA for the considered large nozzles were higher in comparison to results from the Hiroyasu and Arai
 268 model. Auto ignition of the air-fuel mixture in the cylinder of the marine engine occurs when the fuel spray does not reach
 9 its maximum development parameters. Therefore, it is important to develop a model of the change in the SCA over time.
 0 The first five measurements of SCA were omitted from the analysis due to their great dispersion, probably caused by
 1 measurement inaccuracy. The mentioned measurements results have a large error due to the difficulties in processing the
 2 photographic results. The SCA at the beginning of the course at the time was difficult to estimate. The proposed model
 3 presented in this paper Equation (6) was developed on the basis of dependencies defined by combining terms from existing

274 models. When analyzing the experimental results, one can notice the logarithmic function of the early stage of the
275 evolution of the SCA over time.

276 Using this as the basis, the following proposed model of SCA was formulated:

$$277 \quad SCA = \left[-0.462 \cdot \frac{L}{D} + \sqrt{\Delta P} \cdot \left(\frac{\rho_f}{\rho_g} \right)^{0.2} \right] \ln(t) + (3.17 \cdot \Delta P - 28.067), \quad (6)$$

278 By analyzing all considered cases, the average of relative error of proposed model of SCA over time is 20% for
279 backpressure 3.2 MPa and 17% for backpressure 4.3 MPa.

280 **4 Conclusions**

281 The macrostructure of diesel oil spray from a marine engine injector was characterized using the Mie scattering
282 method. The parameters that were measured were the spray tip penetration (STP) and the spray cone angle (SCA). These
283 parameters were analyzed in terms of three different nozzle diameters and two backpressures 3.2 and 4.3 MPa
284 corresponding to engine operation under half and full loads, respectively. The main theories concerning the influence of
285 the geometric parameters of the injector nozzle on STP and SCA were confirmed:

- 286 - Increasing the diameter D of the injector nozzle or decreasing the ratio $\frac{L}{D}$ (where L is the length of the nozzle)
287 increases the STP and SCA;
- 288 - Changing the backpressure from 3.2 to 4.3 MPa decreases the STP and increases the SCA.

289 The early stage of STP was described based on the Hiroyasu and Arai model. But the proposed model also includes
290 a dependence on $\frac{L}{D}$. Additionally, a model for SCA was developed which assumes a logarithmic dependence of the SCA
291 on time. The average of the relative error of the proposed model from the experimental results was about 18%. The new
292 mathematical models of the fuel spray parameters used in this work were obtained on the basis of experimental work with
293 specific conditions. Therefore, the mathematical models of SCA and early STP are specified for specific conditions such
294 as the geometrical parameters of a marine injector, the injection pressure, and the backpressure into a constant volume
295 chamber.

296

7

8

9

0

301 **References**

302

303 Adamczyk, W.P., Kruczek, G., Bialecki, R. and Przybyła, G. (2020), “Application of different numerical models capable
304 to simulate combustion of alternative fuels in internal combustion engine”, *International Journal of Numerical
305 Methods for Heat and Fluid Flow*, Vol. 30 No. 5, pp. 2517–2534.

306 Balz, R., Nagy, I.G., Weisser, G. and Sedarsky, D. (2021), “Experimental and numerical investigation of cavitation in
307 marine Diesel injectors”, *International Journal of Heat and Mass Transfer*, Elsevier Ltd, Vol. 169, available
308 at:<https://doi.org/10.1016/j.ijheatmasstransfer.2021.120933>.

309 Balz, R., von Rotz, B. and Sedarsky, D. (2020), “In-nozzle flow and spray characteristics of large two-stroke marine
310 diesel fuel injectors”, *Applied Thermal Engineering*, Elsevier, Vol. 180 No. June, p. 115809.

311 Bohl, T., Tian, G. and Smallbone, A. (2017), “Macroscopic spray characteristics of next-generation bio-derived diesel
312 fuels in comparison to mineral diesel”, *Applied Energy*, The Author(s), Vol. 186, pp. 562–573.

313 Cai, G. and Abraham, J. (2017), “Multidimensional simulations of non-reacting and reacting diesel and biodiesel sprays”,
314 *Energy*, Elsevier Ltd, Vol. 119, pp. 1221–1229.

315 Chen, L., Li, G., Huang, D., Zhang, Z., Lu, Y., Yu, X. and Roskilly, A.P. (2019), “Experimental and numerical study on
316 the initial tip structure evolution of diesel fuel spray under various injection and ambient pressures”, *Energy*,
317 Elsevier Ltd, Vol. 186, p. 115867.

318 Feng, Z., Zhan, C., Tang, C., Yang, K. and Huang, Z. (2016), “Experimental investigation on spray and atomization
319 characteristics of diesel / gasoline / ethanol blends in high pressure common rail injection system”, *Energy*, Elsevier
320 Ltd, Vol. 112, pp. 549–561.

321 Grochowalska, J. (2019), “Analysis of the macrostructure of the fuel spray atomized with marine engine injector”,
322 *Combustion Engines*, Vol. 179 No. 4, pp. 80–85.

323 Heywood, J.B. (1988), *Internal Combustion Engine Fundamentals, McGrawHill Series in Mechanical Engineering*, Vol.
324 21, available at:<https://doi.org/10987654>.

325 Hiroyasu, H. and Arai, M. (1990), “Structures of Fuel Sprays in Diesel Engines”, *SAE Technical Paper*.

326 Jing, D., Zhang, F., Li, Y., Xu, H. and Shuai, S. (2017), “Experimental investigation on the macroscopic and microscopic
7 spray characteristics of diesel fuel”, *Fuel*, Elsevier Ltd, Vol. 199, pp. 478–487.

8 Kegl, B. and Lešnik, L. (2018), “Modeling of macroscopic mineral diesel and biodiesel spray characteristics”, *Fuel*, Vol.
9 222, pp. 810–820.

0 Kistler. (2014), *Piezoresistive High Pressure Sensor [Online]*, available at:
1 <https://www.kistler.com/?type=669&fid=61054&model=document&callee=frontend>.

2 Kostas, J., Honnery, D. and Soria, J. (2009), “Time resolved measurements of the initial stages of fuel spray penetration”,

- 333 *Fuel*, Elsevier Ltd, Vol. 88 No. 11, pp. 2225–2237.
- 334 Kowalski, J. (2014), “An experimental study of emission and combustion characteristics of marine diesel engine with
335 fuel pump malfunctions”, *Applied Thermal Engineering*, Elsevier Ltd, Vol. 65 No. 1–2, pp. 469–476.
- 336 Kowalski, J. (2016), “An experimental study of emission and combustion characteristics of marine diesel engine with
337 fuel injector malfunctions”, *Polish Maritime Research*, Vol. 23 No. 1, pp. 77–84.
- 338 Lee, C.S. and Park, S.W. (2002), “An experimental and numerical study on fuel atomization characteristics of high-
339 pressure diesel injection sprays”, *Fuel*, Vol. 81 No. 18, pp. 2417–2423.
- 340 Lei, Y., Liu, J., Qiu, T., Mi, J., Liu, X. and Zhao, N. (2019), “Effect of injection dynamic behavior on fuel spray
341 penetration of common-rail injector”, *Energy*, Elsevier Ltd, Vol. 188, p. 116060.
- 342 Liu, F., Li, Z., Wang, Z., Dai, X., He, X. and Lee, C. (2018), “Microscopic study on diesel spray under cavitating
343 conditions by injecting fuel into water”, Vol. 230 No. October 2017, pp. 1172–1181.
- 344 Naber, J. and Siebers, D.L. (1996), “Effects of Gas Density and Vaporization on Penetration and Dispersion of Diesel
345 Sprays”, No. 412, available at:<https://doi.org/10.4271/960034>.
- 346 Nishida, K., Tian, J., Sumoto, Y., Long, W., Sato, K. and Yamakawa, M. (2009), “An experimental and numerical study
347 on sprays injected from two-hole nozzles for DISI engines”, *Fuel*, Elsevier Ltd, Vol. 88 No. 9, pp. 1634–1642.
- 348 Payri, R., García-Oliver, J.M., Xuan, T. and Bardi, M. (2015), “A study on diesel spray tip penetration and radial
349 expansion under reacting conditions”, *Applied Thermal Engineering*, Elsevier Ltd, Vol. 90, pp. 619–629.
- 350 Payri, R., Salvador, F.J., Gimeno, J. and de la Morena, J. (2009), “Effects of nozzle geometry on direct injection diesel
351 engine combustion process”, *Applied Thermal Engineering*, Elsevier Ltd, Vol. 29 No. 10, pp. 2051–2060.
- 352 Payri, R., Tormos, B., Salvador, F.J. and Araneo, L. (2008), “Spray droplet velocity characterization for convergent
353 nozzles with three different diameters”, *Fuel*, Vol. 87 No. 15–16, pp. 3176–3182.
- 354 Payri, R., Viera, J.P., Gopalakrishnan, V. and Szymkowicz, P.G. (2017), “The effect of nozzle geometry over the
355 evaporative spray formation for three different fuels”, *Fuel*, Elsevier Ltd, Vol. 188, pp. 645–660.
- 356 Piazzullo, D., Costa, M., Allocca, L., Montanaro, A. and Rocco, V. (2017), “Schlieren and Mie scattering techniques for
357 the ECN ‘Spray G’ characterization and 3D CFD model validation”, *International Journal of Numerical Methods
358 for Heat & Fluid Flow*, Vol. 28 No. 2, pp. 498–515.
- 9 Reitz, R.D. and Bracco, F.B. (1979), “On the Dependence of Spray Angle and Other Spray Parameters on Nozzle Design
0 and Operating Conditions”, available at:<https://doi.org/10.4271/790494>.
- 1 Siebers, D.L. (1999), “Scaling liquid-phase fuel penetration in diesel sprays based on mixing-limited vaporization”, *SAE
2 Technical Papers*, No. 724, available at:<https://doi.org/10.4271/1999-01-0528>.
- 3 Som, S., Ramirez, A.I., Longman, D.E. and Aggarwal, S.K. (2011), “Effect of nozzle orifice geometry on spray,
4 combustion, and emission characteristics under diesel engine conditions”, *Fuel*, Elsevier Ltd, Vol. 90 No. 3, pp.

- 365 1267–1276.
- 366 Sou, A., Hosokawa, S. and Tomiyama, A. (2007), “Effects of cavitation in a nozzle on liquid jet atomization”,
367 *International Journal of Heat and Mass Transfer*, Vol. 50 No. 17–18, pp. 3575–3582.
- 368 Suh, H.K., Park, S.W. and Lee, C.S. (2007), “Effect of piezo-driven injection system on the macroscopic and microscopic
369 atomization characteristics of diesel fuel spray”, *Fuel*, Vol. 86 No. 17–18, pp. 2833–2845.
- 370 Vaid, H.S., Singh, K.D., Lou, H.H., Chen, D. and Richmond, P. (2014), “A run time combustion zoning technique towards
371 the EDC approach in large-scale CFD simulations”, *International Journal of Numerical Methods for Heat and Fluid
372 Flow*, Vol. 24 No. 1, pp. 21–35.
- 373 Wang, X. (2013), “A phenomenological bubble number density model developed for simulation of cavitating flows inside
374 high-pressure diesel injection nozzles”, *International Journal of Numerical Methods for Heat & Fluid Flow*, Vol.
375 23 No. 8, pp. 1356–1372.
- 376 Wang, X., Wang, X., Zhang, J. and Wang, J. (2015), “Nozzle Diameter Influence on Spray characteristics in a Constant
377 Volume Combustion Chamber”, *Mathematical Modelling of Engineering Problems*, Vol. 2 No. 3, pp. 9–12.
- 378 Wang, Z., Ding, H., Ma, X., Xu, H. and Wyszynski, M.L. (2016), “Ultra-high speed imaging study of the diesel spray
379 close to the injector tip at the initial opening stage with single injection”, *Applied Energy*, Elsevier Ltd, Vol. 165,
380 pp. 335–344.
- 381 Yan, F., Du, Y., Wang, L., Tang, W., Zhang, J., Liu, B. and Liu, C. (2016), “Effects of injection pressure on cavitation
382 and spray in marine diesel engine”, *International Journal of Spray and Combustion Dynamics*, Vol. 0 No. 2, pp. 1–
383 13.
- 384 Yao, C., Geng, P., Yin, Z., Hu, J., Chen, D. and Ju, Y. (2016), “Impacts of nozzle geometry on spray combustion of high
385 pressure common rail injectors in a constant volume combustion chamber”, *Fuel*, Elsevier Ltd, Vol. 179, pp. 235–
386 245.
- 387 Yu, W., Yang, W., Mohan, B., Tay, K.L. and Zhao, F. (2017), “Macroscopic spray characteristics of wide distillation fuel
388 (WDF)”, *Applied Energy*, Elsevier Ltd, Vol. 185, pp. 1372–1382.
- 389 Yu, Y. (2019), “Experimental study on effects of ethanol-diesel fuel blended on spray characteristics under ultra-high
390 injection pressure up to 350 MPa”, *Energy*, Elsevier Ltd, Vol. 186, p. 115768.
- 1 Zhou, X., Li, T., Wei, Y. and Wu, S. (2019), “Scaling spray combustion processes in marine low-speed diesel engines”,
2 *Fuel*, Elsevier, Vol. 258 No. September, p. 116133.
- 3 Zigan, L., Schmitz, I., Flügel, A., Wensing, M. and Leipertz, A. (2011), “Structure of evaporating single- and
4 multicomponent fuel sprays for 2nd generation gasoline direct injection”, *Fuel*, Elsevier Ltd, Vol. 90 No. 1, pp.
5 348–363.
- 6